Three-State, Conformational Probe for Hydrophobic, π-Stacking Interactions in Aqueous and Mixed Aqueous Solvent Systems: Anisotropic Solvation of Aromatic Rings

Milind D. Sindkhedkar, Hormuzd R. Mulla, and Arthur Cammers-Goodwin*

Contribution from the Department of Chemistry, University of Kentucky, Lexington, Kentucky 40506

Received January 31, 2000. Revised Manuscript Received July 19, 2000

Abstract: The conformational equilibrium of α,α′-*m*-xylylene-*N*,*N*′-bis-2-phenylpyridinium (**1a**) is analyzed as a three-state system and is herein proposed as a minimalist conformational probe to assay the stability of hydrophobic aromatic clusters in aqueous and mixed aqueous solvents. VT NMR spectrometry and computation elucidate the dynamic behavior of the conformational distribution of **1a**. In this analysis the effect of diamagnetic anisotropy of the phenyl rings on the central *m*-xylene ring plays a vital role. α,α′-*m*-Xylylene-*N*,*N*′-bis-2-methylpyridinium (**1b**) serves as a spectrometric and calculational reference. Low aqueous concentrations of MeOD-d_4, EtOD-d_6, *i*PrOD-d_8, HFIP-d_2, HFA-d_2, and DMSO-d_6 perturb the distribution of conformers of **1a** observed in D_2O. With fluoroalkanol as cosolvent, the conformer (C) that hides the most hydrogen atom SASA is the most stable. With alkanol as cosolvent, the conformer (F) that exposes the most hydrogen atom SASA is most stable. The work suggests a solvent parameter based on conformation that places water between alkanol and fluoroalkanol. Studies indicate that perturbations from pure aqueous solvation by HFIP or HFA (2−10 mol %) enhance the hydrophobicity (solvophobicity) of the solute (or lipophobicity of the solvent) primarily by increasing ΔH of solvation. Results are discussed in terms of anisotropic solvation of aromatic rings, perturbations by cosolvent, and exalted hydrophobic interactions between aqueous solvent and solute when the solute bears charge. Significance of the work is drawn to the solvent effect on peptide conformation.

In recent years abiotic, minimalist models for canonical, noncovalent interactions such as hydrogen bonding, hydrophobic/solvophobic packing,[1−3] and aqueous π-stacking[4−10] have been used to describe the contributions of these structural features to the molecular properties of large biological molecules. Studies of minimalist canonical interactions also contribute to our ability to design small-molecule drugs for biological targets. Here we use a minimalist conformational model to describe hydrophobic effects on π-stacking in mostly aqueous solutions. We are particularly interested in how aqueous mixtures of fluoroalkanols impact solvated hydrocarbon because this relates directly to many studies of peptide conformation.[11] For many solutes incapable of hydrogen bonding, ΔH and ΔS of transfer from organic to aqueous solution correlate well with the solvent accessible surface area (SASA) of solutes.[12] Major questions to answer in relating the hydrophobic effect to solvent-dependent conformational changes are what is the minimal loss in SASA due to conformational shift necessary to model hydrophobic packing and what types of SASA or aqueous solvent conditions optimally unveil these effects? This work provides partial answers to these questions.

Chart 1[a]

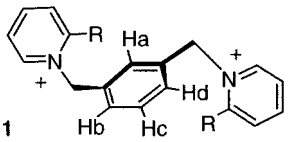

1

[a] **1a**: R = Ph. **1b**: R = Me.

Magnetic anisotropy is used to observe changes in the conformation of **1a** (Chart 1) as a function of solvent and temperature. Diamagnetic anisotropy has been used in the conformational analysis of semiflexible molecules.[13−17] However, the use of ab initio calculations of chemical shift perturbations based on a reference molecule described in this and a preceding paper is novel.[18] Furthermore, the conformers of **1a** exchange quickly on the NMR time scale; usually

(1) Smithrud, D. B.; Diederich, F. *J. Am. Chem. Soc.* **1990**, *112*, 339−343.
(2) Gardner, R. R.; Christianson, L. A.; Gellman, S. H. *J. Am. Chem. Soc.* **1997**, *119*, 5041−5042.
(3) Nelson, J. C.; Saven, J. G.; Moore, J.; Wolynes, P. G. *Science* **1997**, *277*, 1793.
(4) Newcomb, L. F.; Gellman, S. H. *J. Am. Chem. Soc.* **1994**, *116*, 4993−4994.
(5) Newcomb, L. F.; Haque, T. S.; Gellman, S. H. *J. Am. Chem. Soc.* **1995**, *117*, 6509−6519.
(6) Pang, Y. P.; Miller, J. L.; Kollman, P. A. *J. Am. Chem. Soc.* **1999**, *121*, 1717−1725.
(7) Kim, E.-I.; Paliwal, S.; Wilcox, C. S. *J. Am. Chem. Soc.* **1998**, *120*, 11192−11193.
(8) Breinlinger, E. C.; Rotello, V. M. *J. Am. Chem. Soc.* **1997**, *119*, 1165−1166.
(9) Matray, T. J.; Kool, E. T. *J. Am. Chem. Soc.* **1998**, *120*, 6191−6192.
(10) Kool, E. T.; Morales, J. C.; Guckian, K. M. *Angew. Chem., Int. Ed. Engl.* **2000**, *39*, 990−1009.
(11) Buck, M. *Q. Rev. Biophys.* **1998**, *31*, 297.
(12) Gill, S. J.; Dee, S. F.; Olafson, G.; Wadsö, I. *J. Phys. Chem.* **1985**, *89*, 3758−3761.
(13) Schladetzky, K. D.; Haque, T. S.; Gellman, S. H. *J. Org. Chem.* **1995**, *60*, 4108−4113.
(14) Lofthagen, M.; Siegel, J. S. *J. Org. Chem.* **1995**, *60*, 2885−2890.
(15) Fukazawa, Y.; Yang, Y.; Hayashibara, T.; Usui, S. *Tetrahedron* **1996**, *52*, 2847−2862.
(16) Fukazawa, Y.; Usui, S.; Tanimoto, K.; Hirai, Y. *J. Am. Chem. Soc.* **1994**, *116*, 8169−8175.
(17) Fukazawa, Y.; Hayashibara, T.; Yang, Y.; Usui, S. *Tetrahedron. Lett.* **1995**, *36*, 3349−3352.

10.1021/ja0003270 CCC: $19.00
Published on Web 09/07/2000

investigators employ hindered, two-state systems to use NMR integration.[2,7]

Deviations from pure aqueous conditions strongly influence the conformational preference of small molecules when the solvent-accessibilities of hydrogen bond donors or acceptors differ in two or more competing conformers.[19−22] In the absence of these structural features, the conformational preferences of small flexible molecules are usually solvent independent. In particular, conformational dependence on the hydrophobic effect is not pronounced in small molecules. However, in proteins and other polymers hydrophobic collapse controls conformation.[5,23−27] The hydrophobic effect has been described as the maximization of entropy of hydration on the part of flexible molecules by a general shift toward conformers that remove hydrocarbon from water.[28] Despite the focus on ΔS, mathematical models for liquid water systems call attention to enthalpic as well as entropic interactions between solvent and solute.[25,26,29−34]

The terms hydrophobic and solvophobic should be interchangeable in this study because the solvent mixtures were mostly aqueous. The former term is a subset of the latter. Hydrophobic is solvophobic when water is the solvent; both terms refer to unfavorable interaction between solvent and solute. What would happen to the hydrophobic effect if water (in the solvent shell) were to become more cohesive without compensating interactions between water and solute? Multiply charged quaternary salts might be an example of this situation. In the presence of strongly polar or charged species, water/water interactions in the aqueous solvent shell become stronger and the liquid state near the solute becomes denser.[35] The situation can be framed in terms of "salting out" at the microscopic level.[36−38] Computation supports this concept on the scale of biological molecules.[39,40] Furthermore, dipole-induced structuring of the aqueous solvent shell has been proposed regarding peptide conformation in a nonconventional view of the hydrophobic effect.[41] Charge-induced or dipole-induced changes by solute on aqueous solvent shells may offer a method to drive conformational preference with minimalist hydrophobic interactions. Thus, increasing conformer-specific ΔH between solute and solvent or decreasing ΔS of solvation (from solvent-shell structure) should render hydrophobic collapse more favorable and hence more observable in small molecules.

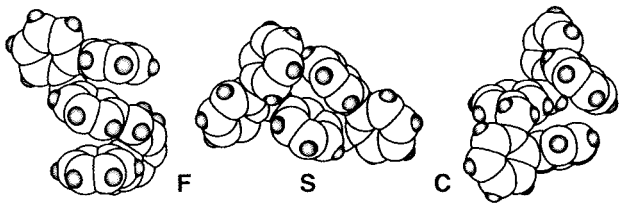

Figure 1. Compound **1a** shown in three canonical conformers: the face-to-face, center-to-edge stacked conformer, F, the splayed conformer, S, and the cluster conformer, C. All three structures above were generated with MM2* in Macromodel V4.5 with conformational searching and GB/SA water simulation. The first 50 conformers found were within 0.8 kcal of each other and each was a member of the three families of conformers represented by F, S, and C. The crystal structure of **1a** most resembled the F conformer. In the calculated structures, S had only one ring splayed. C was the MM2* global minimum.

This work probes the nature of the solvation of aromatic hydrocarbon when water is perturbed with small amounts of alcoholic cosolvent. A detailed study of the three-state conformational equilibrium of α,α′-*m*-xylylene-*N*,*N*′-bis-2-phenylpyridinium dibromide (**1a**) is described. The effect of diamagnetic anisotropy of the phenyl rings on the ^{1}H chemical shifts of the xylene ring in **1a** changes markedly with conformation. Conformer-specific chemical shift tensors and measurement of chemical shifts provide enough information to determine the mole fractions of three families of conformers, F, S, and C (see Figures 1 and 2). The major difference between the conformers of **1a** in terms of solvent-accessible surface area (SASA) is F exposes the most hydrogen atom SASA, C exposes the most carbon atom SASA, and S exposes an intermediate amount of each type of SASA. Water stabilizes the three conformers nearly equally and very low energy barriers allow facile exchange between conformers. Studies of the relative solution stabilities and thermodynamic analyses of the three-state system allow generalizations regarding the effect of low concentrations of aqueous cosolvents on atomistic SASA. The difference between water and other solvents regarding stacked (conformer F and C) versus unstacked conformers (conformer S) is less than would be expected if π-stacking were driven strongly by the hydrophobic effect. This notion has been previously expressed[42] and has generated controversy.[43] Significance of the current studies is drawn to anisotropic solvation of aromatic moieties, fluoroalkanol-induced peptide conformation, and the hydrophobic effect.

Results and Discussion

Chemical Shifts and Conformers of 1a. To use **1a** as a conformational probe of solvation, the solvent-sensitive behavior of the chemical shifts of **1a** needed to be correlated with changes in conformation. This was a daunting task because conformational change in **1a** was fast on the NMR time scale. Monte Carlo conformational searching (Macromodel 5.0, MM2*, GB/SA solvation)[44] indicated that conformers that positioned the

(18) Mulla, H. R.; Cammers-Goodwin, A. *J. Am. Chem. Soc.* **2000**, *122*, 738−739.
(19) Perrin, C. L.; Babian, M. A.; Rivero, I. A. *J. Am. Chem. Soc.* **1998**, *120*, 1044.
(20) Urban, J. J.; Cronin, C. W.; Famini, G. R. *J. Am. Chem. Soc.* **1997**, *119*, 12292.
(21) Eguchi, T.; Kondo, K.; Kakinuma, K.; Uekusa, H.; Ohashi, Y.; Mizoue, K.; Qiao, Y. F. *J. Org. Chem.* **1999**, *64*, 5371−5376.
(22) Carlson, H. A.; Jorgensen, W. L. *J. Am. Chem. Soc.* **1996**, *118*, 8475.
(23) Kauzmann, W. *Adv. Protein Chem.* **1959**, *14*, 1−62.
(24) Brive, L.; Dolphin, G. T.; Baltzer, L. *J. Am. Chem. Soc.* **1997**, *119*, 8598−8607.
(25) Lee, B.; Graziano, G. *J. Am. Chem. Soc.* **1996**, *118*, 5163−5168.
(26) Silverstein, K. A. T.; Haymet, A. D. J.; Dill, K. A. *J. Am. Chem. Soc.* **1998**, *120*, 3166−3175.
(27) Hecht, D.; Tadesse, L.; Walters, L. *J. Am. Chem. Soc.* **1992**, *114*, 4336−4339.
(28) Haymet, A. D. J.; Silverstein, A. T.; Dill, K. A. *Faraday Discuss.* **1996**, *103*, 117−124.
(29) Lubineau, A.; Augé, J. *Top. Curr. Chem.* **1999**, *206*, 1−39.
(30) Muller, N. *Acc. Chem. Res.* **1990**, *23*, 23−28.
(31) Silverstein, K. A. T.; Haymet, A. D. J.; Dill, K. A. *J. Chem. Phys.* **1999**, *111*, 8000−8009.
(32) Lee, B. *Biophys. Chem.* **1994**, *51*, 271−278.
(33) Mancera, R. L.; Kronberg, B.; Costas, M.; Silveston, R. *Biophys. Chem.* **1998**, *70*, 57−63.
(34) Graziano, G. *J. Chem. Soc., Faraday Trans.* **1998**, *94*, 3345−3352.
(35) Kanno, H.; Ohnishi, A.; Tomikawa, K.; Yoshimura, Y. *J. Raman Spectrosc.* **1999**, *30*, 705−713.
(36) Mancera, R. L. *Chem. Phys. Lett.* **1998**, *296*, 459−465.
(37) Mancera, R. L. *J. Phys. Chem. B* **1999**, *103*, 3774−3777.
(38) Rosas-García, V. M.; Gandour, R. D. *J. Am. Chem. Soc.* **1997**, *119*, 7587−7588.
(39) Lum, K.; Chandler, D.; Weeks, J. D. *J. Phys. Chem. B* **1999**, *103*, 4570−4577.
(40) Wilson, E. K. *Chem. Eng. News* **1999**, *Aug 2*, 24−25.
(41) Walgers, R.; Lee, T. C.; Cammers-Goodwin, A. *J. Am. Chem. Soc.* **1998**, *120*, 5073−5079.
(42) Gellman, S. H.; Haque, T. S.; Newcomb, L. F. *Biophys. J.* **1996**, *71*, 3523−3525.
(43) Friedman, R. A.; B., H. *Biophys. J.* **1996**, *71*, 3525−3526.

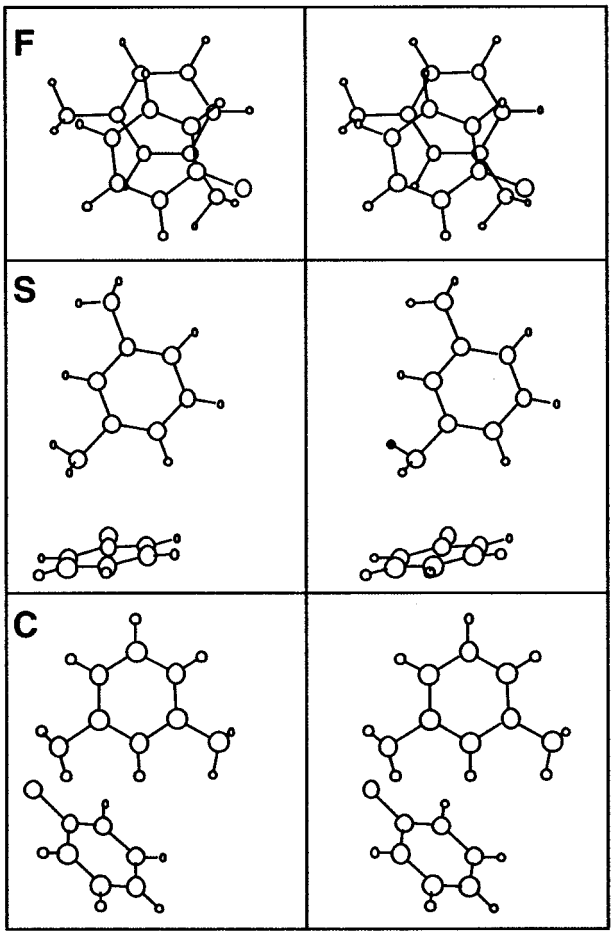

Figure 2. Stereoviews of two-ring conformers of F, S, and C. Atoms were stripped from **1a** to leave fragments of toluene and xylene while preserving spatial relationships between the two rings. Since **1a** is dynamically symmetric about the plane containing the xylene ring a quick glance at the stereoviews should convince the reader that C allows three ring interactions, whereas F allows only two-ring interactions. These atomic coordinates were used to perform calculations of the chemical shift tensors. Another set of three calculations on xylene/ethane fragments modeled chemical shifts in **1b**.

pyridinium rings on the same side of the *m*-xylene moiety in **1a** were electrostatically and sterically destabilized. Thus the amount of allowed conformers was greatly decreased. The first 50 conformers (all within 0.8 kcal/mol) fell into three classes. These states were abbreviated F (face-to-face, edge-to-center π-stacking), S (splayed), and C (cluster), respectively (see Figure 1). The conformational description of **1** was dynamically symmetric with respect to the plane containing the *m*-xylene moiety and was modeled with a two-ring analysis. A three-ring analysis would have given rise to six states explicitly, instead of three mixed states; however, the ^{1}H NMR spectra of **1a** did not contain enough information to explicitly define six states. F, S, and C are sets of conformers consisting of structurally related microstates. Figure 2 shows stereoviews of the three canonical two-ring states F, S, and C from a perspective perpendicular to the xylene ring. F was the conformer in which **1a** crystallized.[18] Only two of the three all-carbon rings could interact simultaneously in F. Conformers F and S were dynamically symmetrical with respect to Ha and Hb in the model used here. However in S, the phenyl ring did not stack on the xylene ring even though mixed S states permitted loose, 3-ring interactions between the xylene and the two phenyl rings (see Figure 1). Unlike S and F the phenyl rings in the C conformer could strongly interact and diamagnetically shifted δ_{Ha} more than δ_{Hb}.

Determination of the conformational propensity of **1a** by diamagnetic anisotropy required a reference compound in the calculation of chemical shift tensors at Ha, Hb, and Hc. In the experimental NMR work a reference compound was used to account for the effect of bulk solvent on the chemical shift in the absence of the diamagnetic anisotropy due to the phenyl rings. An ideal reference compound was *bis*-picoline derivative **1b**. If electrostatic interactions controlled the conformation of **1a** and **1b** similarly, the magnetic anisotropy of the pyridinium rings should have affected the chemical shifts in the *m*-xylene ring similarly in both molecules. Differences in inductive effect on Ha and Hb between methyl in **1b** and phenyl in **1a** should have been minimal since six bonds separated these protons from the substitution site. Thus, **1b** should have corrected for the effect of bulk solvent on the chemical shifts of Ha, Hb, and Hc in **1a**.

The three-state conformational equilibrium of **1a** was modeled with two-ring chemical shift tensors of the canonical conformers: F, S, and C. Combining calculations, mass balance, and ^{1}H NMR experimental results gave rise to the following three equations for three unknowns:

$$\Delta\delta_{Ha}\mathbf{1b}-\mathbf{1a} = 0.88X_F + (-0.04)X_S + 1.96X_C \quad (1)$$

$$\Delta\delta_{Hb}\mathbf{1b}-\mathbf{1a} = 0.88X_F + (-0.04)X_S + 0.14X_C \quad (2)$$

$$X_F + X_S + X_C = 1 \quad (3)$$

In eqs 1−3, $\Delta\delta_{Ha}$**1b**−**1a** means the chemical shift of Ha in compound **1a** subtracted from the chemical shift of Ha in compound **1b**; these values were determined with two separate ^{1}H NMR measurements of **1a** and **1b** under identical conditions. X_F, X_S, and X_C are the mole fractions of the canonical conformers described above. The constants in eqs 1 and 2 are chemical shift tensors due to anisotropies of the phenyl rings in F, S, and C; these have been obtained from DFT calculations of chemical shifts in abbreviated structures of **1a** and **1b** in F, S, and C (see Figure 2). For **1a** two-ring fragments of toluene and xylene were used; for **1b** fragments of ethane and xylene were used. Recent studies have optimized the calculation of ^{1}H NMR chemical shifts.[45] DFT calculations applied to the two-ring canonical structures shown in Figure 2 have been recently described.[18]

Solvent-Sensitive Conformational Preference. Figure 3 shows raw data and compares spectra of **1a** to spectra of **1b** in 20 mol % *i*PrOD versus 7.5 mol % HFA. To describe how the conformational preference of **1a** changes with solvent, cosolvent (containing equimolar **1a** or **1b**) was sequentially added to NMR samples of **1a** and **1b** in D_2O at constant temperature. This work focused on perturbations of aqueous solvation so the abbreviated titrations in Figures 4−6 confined the experiments to the region of greatest change and greatest interest. X_C, X_F, and X_S in pure solvents were reported previously.[18] Increasing cosolvent concentrations beyond those in Figures 4−6 did not result in major redistribution of X_C, X_F, or X_S. Thus the end points of the curves in Figures 4−6 were similar to the conformational preferences in the pure solvents.

(44) Mohamadi, F.; Richards, N. G. J.; Guida, W. C.; Liskamp, R.; Lipton, M.; Caufield, C.; Chang, G.; Hendrickson, T.; Still, W. C. *J. Comput. Chem.* **1990**, *11*, 440.

(45) Cheeseman, J. R.; Trucks, G. W.; Keith, T. A.; Frisch, M. J. *J. Chem. Phys.* **1996**, *104*, 5497−5509.

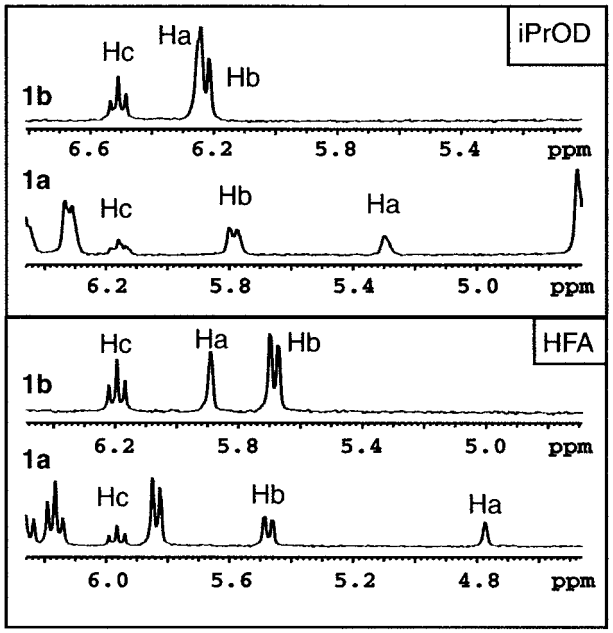

Figure 3. Stacked ^{1}H NMR spectra comparing the *m*-xylyl chemical shifts of **1a** to those of **1b** in 20.3 mol % ^{i}PrOD (top) versus 7.46 mol % HFA (bottom). Note that $\Delta\delta_{Hc}$**1b**−**1a** is ∼0.34 ppm in *i*PrOD solution versus ∼0.22 ppm in HFA solution. This slight rise was predicted by the tensor as F increased in population. However changes in $\Delta\delta_{Hc}$**1b**−**1a** from solvent to solvent were too small to be of diagnostic value. Decreasing differences between $\Delta\delta_{Ha}$**1b**−**1a** and $\Delta\delta_{Hb}$**1b**−**1a** on going from HFA to *i*PrOD indicated that the conformational distribution progressed from mostly C to mostly F because the phenyl effect of diamagnetic anisotropy on Ha and Hb became more symmetric.

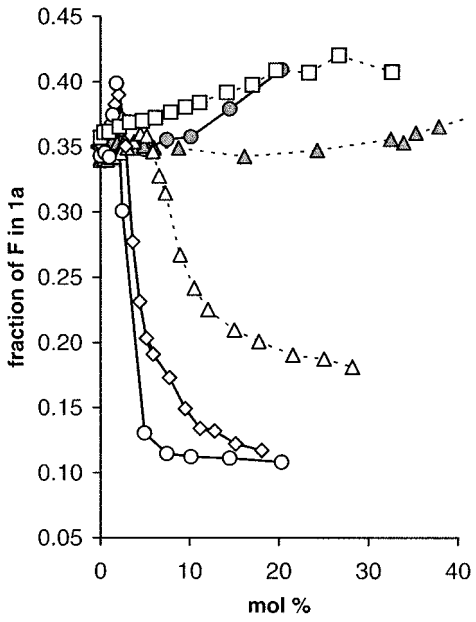

Figure 4. Solvent sensitive X_F. Scales on the axis and the legends of Figures 4−6 are identical.

From Figures 4−6 it is evident that the alkanols shifted the conformational preference of **1a** differently than the fluoroalkanols. Divergent behavior of **1a** with these two classes of alcohols was the first clue that hydrophobic interactions mandated the conformation. Hydrophilic probes behaved similarly in the presence of *i*PrOD and HFIP.[41] Furthermore, large alcohols (*i*PrOD) greatly perturbed the conformational preference of **1a** at an earlier stage in the titration than small alcohols (MeOD, EtOD). DMSO primarily behaved like EtOD (note

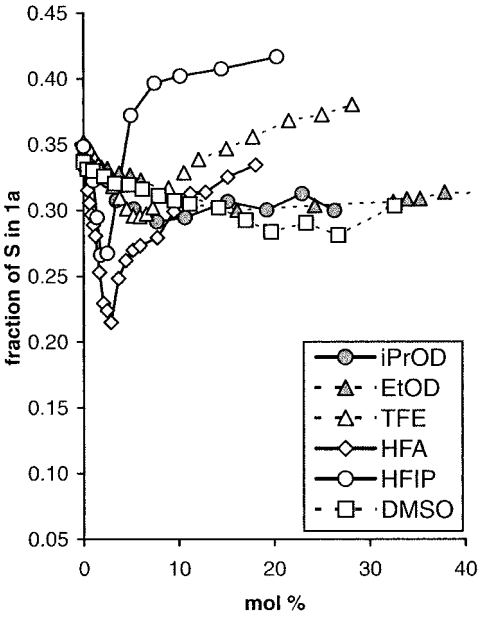

Figure 5. Solvent sensitive X_S. Scales on the axis and the legends of Figures 4−6 are identical.

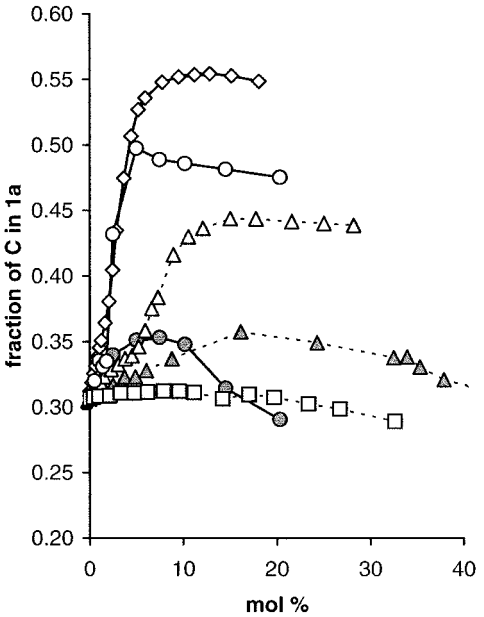

Figure 6. Solvent sensitive X_C. Scales on the axis and the legends of Figures 4−6 are identical.

behavior of F), and this provided direct evidence for the independence of the solvent effect on the hydrogen bond donor ability of the cosolvent. Mass exchanged primarily between X_C and X_F, while X_S varied less with cosolvent. The modest solvent sensitivity of X_S probably reflected the fact that mixed conformers of S had structural properties common to both F and C states (see Figure 1).

Solvent-Accessible Surface Area. Figure 7 gives a qualitative appreciation for the dependence of SASA on the conformation of **1a**. Comparisons of SASA were made by defining atomic sets and calculating SASA with a 1.5 Å solvent probe radius in Macromodel V5.0. Figure 8 shows the percent difference in SASA for various atom types on going from F to C and from F to S states. When SASA of all atoms in C, F, or S was compared, the differences were less than 5%. Changes in volume were also modest. However, when the analysis focused on the hydrogen atoms, the changes in SASA were more dramatic.

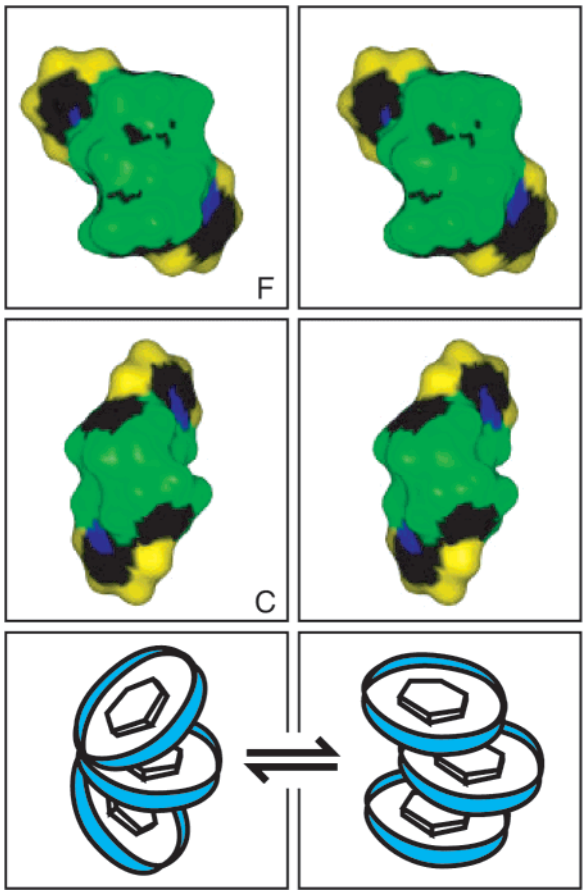

Figure 7. Stereoview of SASA in F versus C. In C, Ha faces toward the reader and in F Ha faces away from the reader; the views are analogous because both structures present the phenyl rings toward the reader. Py and Ph hydrogen atoms (defined in Figure 8) are yellow and green, respectively. Carbon and nitrogen atoms are black and blue, respectively. Illustrations were made with MSI Weblab viewerlite v3.20 with a 1.5 Å solvent-probe radius. The equilibrium between C (left) and F (right) for **1a** is caricaturized to show the mechanism of the gain in hydrogen atom SASA on going from C to F. The blue rims represent aryl hydrogen atom SASA.

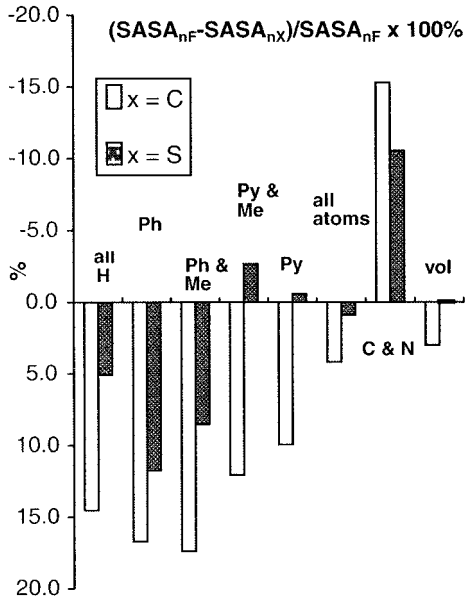

Figure 8. The percent losses in atomistic SASA in calculated structures on going from F to C states and from the F to S states respectively. Negative values on the plot signify increases in SASA on going from F to C or F to S. Ph indicates hydrogen atoms on the benzene rings (not pyridine rings), Me indicates the hydrogen atoms on methylene. Py indicates the hydrogen atoms on the pyridinium ring. Vol indicates the volume of the entire molecule. The X-ray structure was more compact than the calculated structures. When the X-ray structure of F was used, the percent change in SASA in the all atom category was only 1.6%, and the % loss in SASA in other atom types also decreased.

SASA on an atomistic level predicts solvent-dependent properties better than total SASA.[46] Relative to F, C packed the hydrocarbon edges of **1** together and exposed the flat carbon surfaces. In Figure 8, the relatively modest solvent sensitivity of X_S versus X_C and X_F loosely correlated with hydrogen atom ΔSASA.

Thermodynamics of Conformational Distribution. From the graphs of the solvent-dependent $X_{C,S,F}$ of **1a** in Figures 4−6, interesting points were chosen at which to explore entropic versus enthalpic contributions to conformational stability with VT ^{1}H NMR and eqs 1−3. Standard implementation of the van't Hoff equation[47] was used to determine the ΔH and ΔS terms for each conformer. In this analysis the equilibrium constant for the formation of C was defined by the equation $K_C = X_C/(1 - X_C)$; analogous equations were applied to X_F and X_S. Bear in mind when considering Figure 9 that ΔH and $-T\Delta S$ are not on an absolute scale from one solvent to another. Experimentation did not quantify changes in energy of **1a** as a function of solvent. Thus in Figure 9, ΔH_F in one solvent subtracted from ΔH_F in another solvent is not ΔH of transfer of F from one solvent to another. With this caveat in mind, it is instructive to compare the *relative* enthalpic and entropic stabilities of F, S, and C as a function of solvent. Notably, ΔH_F varied more than ΔH_C or ΔH_S with cosolvent with a maximum observed at 8% HFIP. Other notable points in Figure 9 are the favorable ΔH_C and unfavorable ΔS_C. This reflected greater intramolecular interaction and less mobility in C versus F or S; both F and S had positive ΔH terms in water. Solvent-insensitive and temperature-insensitive conformational preference of *N*-benzyl-2-phenylpyridinium derivatives[48] can be retrospectively explained by the thermodynamic analysis of **1a**. These molecules had only F and S conformers and these states had similar relative ΔH terms. The tendency of the aromatic rings in C to cohere found analogy in the exalted interaction in the gas-phase benzene trimer over the benzene dimer[49] and the preference for edge-to-face instead of face-to-face stacking.

ΔH_C, ΔS_C, and ΔG_C at 90 mol % *i*PrOD were not reported because X_C was small (0.10) under these conditions, and upon heating X_C became zero within experimental error. This behavior produced high errors in ΔH_C and ΔS_C. Upon addition of 90 mol % *i*PrOD, ΔH_F became stabilizing (see Figure 9). This fact correlated with the relatively high, aromatic-hydrogen SASA of the F state and the expected favorable dispersive interaction between hydrocarbon in *i*PrOD cosolvent and the aromatic rim of **1a**. Increasing ΔH_F on going from 90 to 0 mol % *i*PrOD can be conceptualized as progressing toward more lipophobic solvent. Likewise, further increasing ΔH_F with increasing concentration of HFIP reaffirmed the characterization of solutes in low concentrations of aqueous fluoroalkanol as solvophobic compared to water[50] and correlated with expected unfavorable interaction between fluorocarbon and the hydrocarbon edge of

(46) Masuda, T.; Jikihara, T.; Nakamura, K.; Kimura, A.; Takagi, T.; Fujiwara, H. *J. Pharm. Sci.* **1997**, *86*, 57−63.
(47) Maskill, H. *Physical Basis of Organic Chemistry*; Oxford University Press: Oxford, UK, 1986.
(48) Martin, T.; Obst, U.; Rebek, J. *Science* **1998**, *281*, 1842−1845.
(49) Henson, B. F.; Venturo, V. A.; Hatland, G. V.; Felker, P. M. *J. Chem. Phys.* **1993**, *98*, 8361−8369.

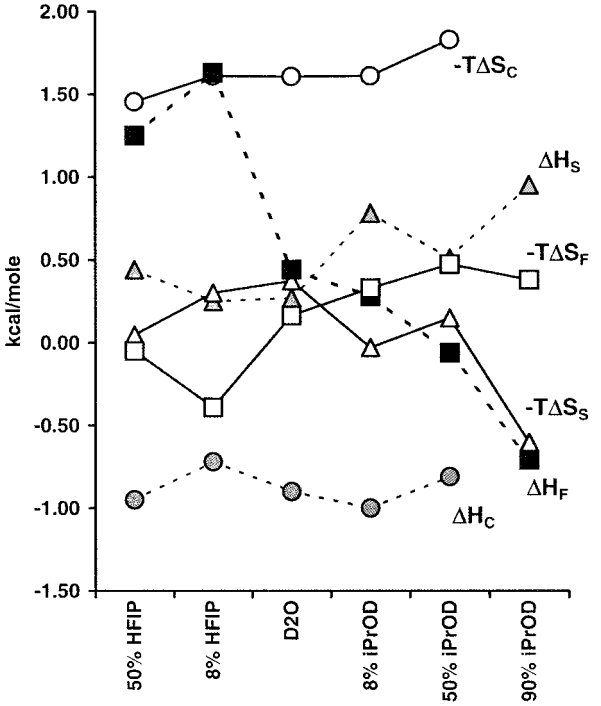

Figure 9. Graph of thermodynamic contributions to $\Delta G_{F,S,C}$ as a function of solvent. The reader is urged to start at D_2O and scan to the right and then to the left. Squares represent F, circles C, and triangles S. The solid icons represent ΔH and the empty icons represent $-T\Delta S$. The precision in kcal/mol is ~0.05. This number was obtained by averaging the standard errors in the slopes and intercepts of the Van't Hoff relationship for all ΔH and $-T\Delta S$ determined. A greater appreciation for the low error can be obtained from the table submitted in the Supporting Information.

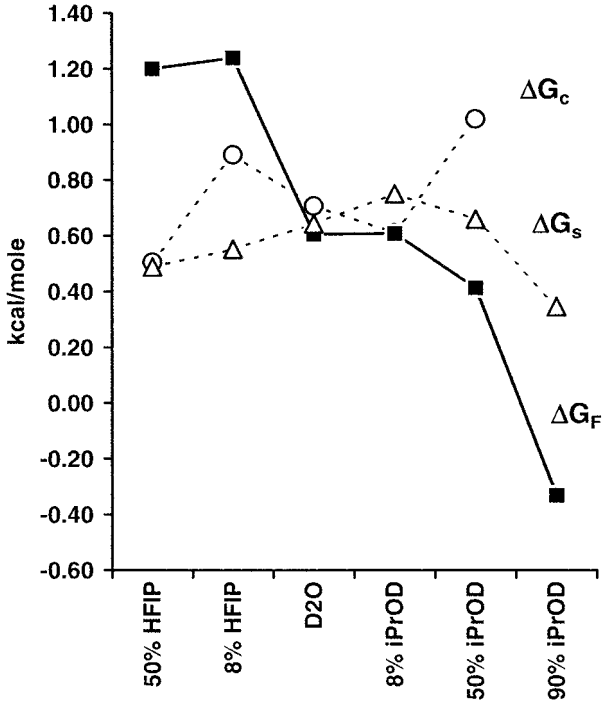

Figure 10. $\Delta G_{F,S,C}$ as a function of solvent. ΔG_C was not reported for 90% *i*PrOD because in this solvent system X_C virtually disappeared from the distribution upon heating. These values of ΔG_C are high and have much error associated with them because the method cannot accurately evaluate small X_C.

the aromatic rings in **1a**.[51] Figure 10 shows that ΔG_F varied the most with changes in solvent and that ΔG_F was determined by ΔH_F (compare Figures 9 and 10). Thus, hydrocarbon SASA in low aqueous concentrations of fluoroalkanol was more hydrophobic (solvophobic) than hydrocarbon SASA in pure water. Combining the SASA analysis and the thermodynamic analysis led to the conclusion that the benzene rings in **1a** were preferentially solvated at the edges instead of the faces. This conclusion was reached because X_F was most solvent-sensitive, alkanol cosolvent stabilized F over the other two states, and F exposed the most hydrogen atom SASA. Proton$-\pi$ interactions could have conceivably caused solvent-sensitive conformation in **1a**;[52] however, the aromatic π-systems in **1a** were probably not electron-rich enough to form hydrogen bonds with the protic solvents used. Furthermore, the similarity of the conformation of **1a** in neat DMSO (electron donor) and pure water (proton donor) does not support the view that proton$-\pi$ interactions were major factors.[18] In support of preferential edge-wise solvation, ab initio calculations recently predicted that significant stabilization is gained from interactions of the form C$-$H$\cdots$ OH_2 with electron-poor organic hydrogen bond donors.[53] Furthermore, molecular dynamics on aqueous benzene indicated that water molecules contact the rims 21 times and the faces 2 times in the first hydration shell.[54] Experimental evidence for these types of unconventional hydrogen bonding interactions was also found in X-ray crystal structures of interactions between macrocyclic ethers and derivatives of paraquat.[55−57] Last, a survey of water molecules around aromatic amino acid residues in protein crystal structures revealed preferential edge-wise interactions between solvent and aromatic groups.[58]

Conclusion

This work establishes that **1a** is the simplest conformational model for hydrophobic cluster interactions (more than two rings) reported to date. Also this study defines a solvent parameter that placed water *between* aqueous mixtures of fluoroalkanol cosolvent and aqueous mixtures of alkanol cosolvent. The effect of charge density of dication **1a** on the immediate aqueous solvent shell is probably a significant factor as this could enhance structure and increase the hydrophobic effect. The lack of interaction (ΔH) between aqueous hydrocarbon solute and fluoroalkanol solvent probably originates from the nonpolarizable C$-$F bonds.[51,59,60]

The drawing at the bottom in Figure 7 caricaturizes the manner in which atomistic SASA was gained on going from C to F. The three benzene rings in the model signify the phenyl and xylyl rings in **1a**. The bands around the aromatic rings signify solvent contact with hydrogen atoms. Separation of these

(50) Andersen, N. H.; Cort, J. R.; Liu, Z.; Sjoberg, S. J.; Tong, H. *J. Am. Chem. Soc.* **1996**, *118*, 10309−10310.
(51) Dunitz, J. D.; Taylor, R. *Chem. Eur. J.* **1997**, *3*, 89−98.
(52) Ma, J. C.; Dougherty, D. A. *Chem. Rev.* **1997**, *97*, 1303−1324.
(53) Gu, Y.; Kar, T.; Scheiner, S. *J. Am. Chem. Soc.* **1999**, *121*, 9411−9422.
(54) Ravishanker, G.; Mehrotra, P. K.; Mezei, M.; Beveridge, D. L. *J. Am. Chem. Soc.* **1984**, *106*, 4102−4108.
(55) Ashton, P. R.; Parsons, I. W.; Raymo, F. M.; Stoddart, J. F.; White, A. J. P.; Williams, D. J.; Wolf, R. *Angew. Chem., Int. Ed. Engl.* **1998**, *37*, 1913−1916.
(56) Bryant, W. S.; Jones, J. W.; Mason, P. E.; Guzei, I.; Rheingold, A. L.; Fronczek, F. R.; Nagvekar, D. S.; Gibson, H. W. *Org. Lett.* **1999**, *1*, 1001−1004.
(57) Meadows, E. S.; De Wall, S. L.; Barbour, L. J.; Fronczek, F. R.; Kim, M.-S.; Gokel, G. W. *J. Am. Chem. Soc.* **2000**, *122*, 3325−3335.
(58) Håkansson, K. *J. Biol. Macromol.* **1996**, *18*, 189−194.
(59) Riess, J. G. *New J. Chem.* **1995**, *19*, 893.
(60) Sadtler, V. W.; Krafft, M. P.; Riess, J. G. *Angew. Chem., Int. Ed. Engl.* **1996**, *35*, 1976.

bands maximizes hydrogen atom SASA. Two groups have probed the effect of hydrophobic interactions on π-stacking in flexible molecules by comparing the effect of DMSO versus water on the conformational preference of aromatic rings linked by water-soluble propylene units.[4,6] Our work suggests that care should be taken in the interpretation of the failure of DMSO to dissociate aromatic moieties that are putatively established by hydrophobic hydration. Equilibria between face-to-face, stacked conformers and unstacked conformers in tethered systems would not greatly change hydrogen atom SASA. These types of conformational equilibria would therefore not be very solvent sensitive. DMSO at 25 mol % stabilized F however, F was a stacked conformer. Furthermore, X_C, X_F, and X_S in neat DMSO were similar to the mole fractions in water.[18] Thus, DMSO does not strongly dissociate aromatic rings that are stacked in water—an observation made previously.[4] Increasing hydrophobicity (solvophobicity) of the solute with small amounts of fluoroalkanol cosolvent appears to be a good protocol to probe stacking interactions; however, caution is required here. In **1a**, fluoroalkanol stabilizes C over F, but both of these are stacked conformers.

The large fluoroalkanols and large alkanols greatly impact the conformation of **1a**, likewise large alkanol cosolvents impact peptide and protein conformation more effectively than small alcohols.[61] Furthermore, α-helices of hydrophobic peptides in modest aqueous concentrations of HFIP[50,62] or HFA[63] undergo cold denaturation—a property usually reserved for large hydrophobic proteins. But how do modest amounts of fluoroalkanol versus alkanol cosolvent impact hydrophobic peptides differently than hydrophilic peptides? From the results above, as the concentration of fluoroalkanol increases, enthalpic stabilization of solvent-exposed hydrocarbon appears to decrease. In this study the difference between $HFIP_{d2}$ and iPrOD$_{d8}$ cosolvent apparently originates from unfavorable enthalpic interactions between fluorocarbon and hydrocarbon versus favorable enthalpic interactions between hydrocarbon and hydrocarbon. By analogy, cold denaturation of hydrophobic peptides in low aqueous concentrations of HFA and HFIP could result from increasing solvophobic interaction between helical conformers and the media as a result of enthalpy not entropy. Observation of cold denaturation requires $\Delta Cp = \delta\Delta H/\delta T \neq 0$; when the ΔH expression in this equation increases, cold denaturation is more observable. Substantial differences in heat capacities necessary for cold denaturation would not occur for any peptide if the enthalpy between random coil and α-helix is small for a given solvent system. Unfortunately experimentation described above does not broach possible differences in heat capacities of conformers C, F, and S; furthermore, the van't Hoff plots are linear.

(61) Hirota, N.; Mizuno, K.; Goto, Y. *J. Mol. Biol.* **1998**, *275*, 365−378.

(62) Andersen, N. H.; Dyer, R. B.; Fesinmeyer, R. M.; Gai, F.; Liu, Z.; Neidigh, J. W.; Tong, H. *J. Am. Chem. Soc.* **1999**, *121*, 9879−9880.

(63) Bhattacharjya, S.; Venkatraman, J.; Kumar, A.; Balaram, P. *J. Pept. Res.* **1999**, *54*, 100−111.

Experimental Section

Synthesis and characterization of **1a** and **1b** have been reported previously. An X-ray structure of **1a**, MS/MS, and elemental analysis for **1a**,**b** were reported.[18] DFT calculations of the chemical shift tensors for use in eqs 1−3 have been described.[18]

All proton NMR studies were carried out between 15 and 20 mM **1**, however, the measurements were largely concentration independent; spectra were recorded at 294−298 K at either 300 or 400 MHz. All deuterated solvents were purchased from commercial sources and used without further purification, except the MeCN-d_3 used in the external reference which was distilled. Spectra recorded in D_2O and mixtures thereof were referenced to an external standard consisting of 3 μL of dioxane in 500 μL of MeCN-d_3 in a sealed glass capillary.

A solution of **1a** or **1b** in the appropriate cosolvent was mixed in aliquots with an equimolar, aqueous solution of the same compound and the ^{1}H NMR was recorded to produce a series of spectra like those in Figure 3. The data were processed with a spreadsheet application to simultaneously solve eqs 1−3. Similar procedures were followed in the VT ^{1}H NMR studies.

Acknowledgment. NSF CHE-9702287 supported this work. Some NMR instruments used in this research were upgraded with funds from the CRIF program of the National Science Foundation (CHE 997841) and from the Research Challenge Trust Fund of the University of Kentucky.

Supporting Information Available: Tabulated data used in Figures 9 and 10 along with the standard errors (PDF). This material is available free of charge via the Internet at http://pubs.acs.org.

JA0003270